Supplementary Material for Elastohydrodynamic Relaxation of Soft and Deformable Microchannels

Gabriel Guyard,[1,2,3] Frédéric Restagno,[3] and Joshua D. McGraw[1,2,*]

[1] *Gulliver CNRS UMR 7083, PSL Research University, ESPCI Paris, 10 rue Vauquelin, 75005 Paris, France*

[2] *IPGG, 6 rue Jean-Calvin, 75005 Paris, France*

[3] *Université Paris-Saclay, CNRS, Laboratoire de Physique des Solides, 91405, Orsay, France*

S.I. LIST OF SYMBOLS

Here we provide a list of symbols appearing in the main text of this Letter.

$A(\tilde{X})$ Spatial part of the separable solution for $\delta P(\tilde{X}, \tilde{T})$

$A_\lambda(\tilde{X})$ Same as $A(\tilde{X})$, the subscript recalls the λ-dependence

$B(\tilde{T})$ Temporal part of the separable solution for $\delta P(\tilde{X}, \tilde{T})$

$B_\lambda(\tilde{T})$ Same as $B(\tilde{T})$, the subscript recalls the λ-dependence

c_0 Capacity of the microfluidic chip inlet

c_1 Magnitude of the pressure-dependent part of c_0

c_2 Magnitude of the constant part of c_0

$\mathcal{C}_\nu(x)$ Linear combination of Bessel functions : $\mathcal{C}_\nu(x) = \mathrm{Y}_{\frac{4}{5}}\left(\frac{8\sqrt{\lambda}}{5}\right)\mathrm{J}_\nu(x) - \mathrm{J}_{\frac{4}{5}}\left(\frac{8\sqrt{\lambda}}{5}\right)\mathrm{Y}_\nu(x)$

d_c Radius of inlet/outlet circles

E^* Effective elastic modulus of the channel material ($E^* \approx E_\mathrm{Y}/0.5427(1-\nu^2)$)

E_Y Young's modulus of the channel material

$h(x,t)$ Local channel height

$H(X,T)$ Dimensionless local channel height ($H = h/h_0$)

h_0 Undeformed channel height

$\mathrm{J}_\nu(x)$ Bessel function of the first kind, of order ν and argument x

L Channel length

$P(X,T)$ Dimensionless pressure field in the channel

$p(x,t)$ Pressure field in the channel

p^* Characteristic pressure scale ($p^* = E^* h_0/w$)

$p_0(t)$ Pressure at chip inlet

$p_{0,\infty}$ Steady-state pressure at chip inlet

$P_{0,\infty}$ Dimensionless, steady-state pressure at chip inlet ($P_{0,\infty} = p_{0,\infty}/p^*$)

$P_\infty(X)$ Dimensionless, steady-state pressure profile in the chip

$p_\mathrm{in}(t)$ Pressure in the reservoir

$p_{\mathrm{in},\infty}$ Steady-state pressure in the reservoir

$q(t)$ Flow rate at chip inlet

q_∞ Steady-state flow rate at chip inlet

Q_∞ Dimensionless steady-state flow rate at chip inlet $Q_\infty = q_\infty r_\mathrm{c}/p^*$

$\mathcal{R}$ Dimensionless inlet resistance defined by $\mathcal{R} = r_0/r_\mathrm{c}$

r_0 Hydraulic resistance of the flow sensor

r_c	Hydraulic resistance of the undeformed channel ($r_\mathrm{c} = 12\eta L/wh_0^3$)
t	Time
T	Dimensionless time ($T = t/\tau_\mathrm{c}$)
$\mathcal{T}$	Dimensionless inlet relaxation time defined by $\mathcal{T} = \tau_0/\tau_\mathrm{c}$
$\tilde{T}$	Rescaled dimensionless time ($\tilde{T} = \Pi^2 T$)
w	Channel width
x	Cartesian coordinate along the length of the channel
X	Dimensionless Cartesian coordinate, along length the length of the channel ($X = x/L$)
$\tilde{X}$	Rescaled dimensionless channel position ($\tilde{X} = \Pi(1 - X) + 1$)
$\tilde{X}_0$	Rescaled channel inlet position, $\tilde{X}_0 = \Pi + 1$
y	Cartesian coordinate along the width of the channel
$\mathrm{Y}_\nu(x)$	Bessel function of the second kind, of order ν and argument x
z	Cartesian coordinate along the height of the channel
α_λ	Integration constant, arising from the resolution of $A_\lambda(\tilde{X})$
β	Prefactor for the asymptotic, power-law description of the Π-dependence of λ_s ($\lambda_\mathrm{s} \approx \beta^2\Pi^\gamma$)
γ	Exponent for the asymptotic, power-law description of the Π-dependence of λ_s ($\lambda_\mathrm{s} \approx \beta^2\Pi^\gamma$)
δp_in	Pressure drop amplitude in the reservoir
$\delta P(X,T)$	Dimensionless excess pressure compared to the steady state ($\delta P(X,T) = P(X,T) - P_\infty(X)$)
η	Fluid viscosity
λ	Eigenvalue of the perturbation analysis
λ_s	Smallest eigenvalue of the perturbation analysis
ν	Poisson's ratio of the channel material
Π	Shifted, dimensionless pressure ($\Pi = (1 + P_{0,\infty})^4 - 1$)
τ_c	Characteristic time scale of the microchannel ($\tau_\mathrm{c} = 12\eta w L^2/h_0^3 E^*$)
τ_t	Transient relaxation time of the microfluidic system
Ω	Volume of fluid stored in the pressure sensor
Ω_a	Volume of air trapped in the pressure sensor

S.II. RAW SIGNALS FOR $p_{\mathrm{in}}(t)$, $p_0(t)$ AND $q(t)$

In Fig. S1 are shown examples of raw signals $p_{\mathrm{in}}(t)$, $p_0(t)$ and $q(t)$. For part (a) is shown the response of a setup containing the flow sensor and pressure controller only. Part (b) displays the response of the full setup containing the pressure controller, flow sensor, pressure sensor and microfluidic chip.

With the flow sensor only, *i.e.* a system without any compliant elements, the response is quasi-instantaneous; in contrast, in the presence of a soft channel and pressure sensor, the system relaxes exponentially to its steady-state upon a pressure change. Exponential fits of the data, shown under the experimental curves in part (b), allow for determinations of τ_{t} and plateau values $p_{0,\infty}$ and q_∞ for each pressure step at the controller.

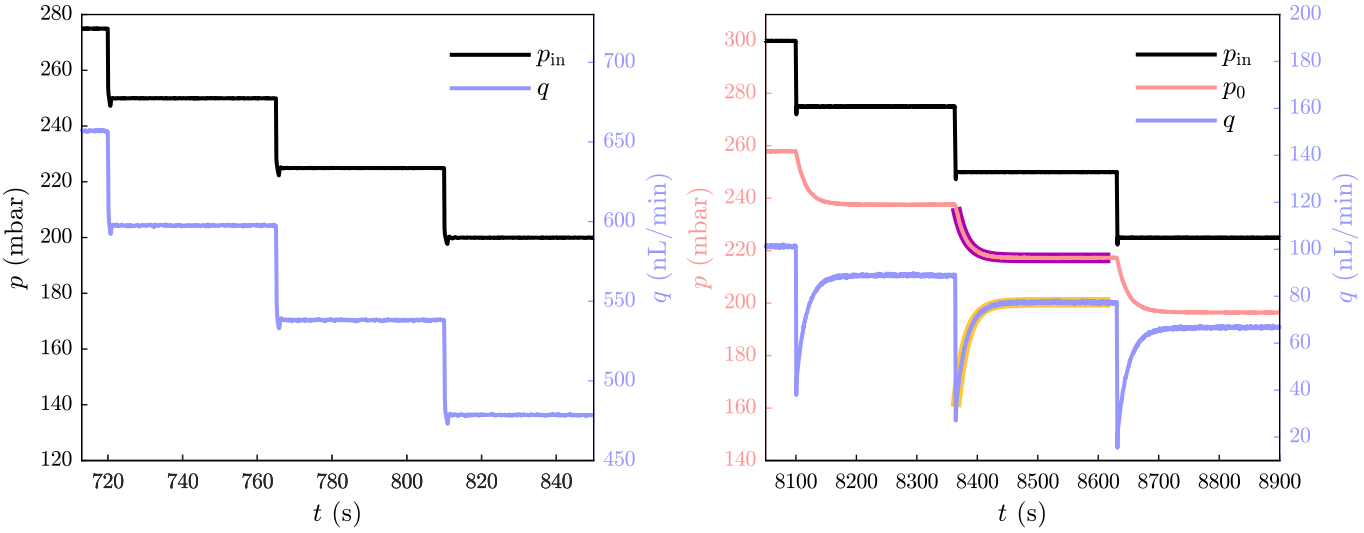

Figure S1. Raw experimental data p_{in}, p_0 and q as a function of time **(a)** without chip connected and **(b)** with a 200 µm-wide chip connected. Thicker lines on **(b)** show exponential fits of the data.

S.III. UNSCALED FLOW-RATE-*VS*-PRESSURE DATA

Figure S2 shows the steady state flow rate q_∞ as a function of the steady state pressure $p_{0,\infty}$, for compliant channels of different width. Unlike the rigid case, the pressure-*vs.*-flow-rate relation is super linear, and can be rationalized with the elastohydrodynamic model described in the main Letter:

$$q_\infty = \frac{p^*}{4r_\mathrm{c}}\left[\left(1+\frac{p_{0,\infty}}{p^*}\right)^4 - 1\right]. \tag{S1}$$

The data are well fitted by this model, as indicated by the solid lines of Fig. S2, which allow to extract an experimental measurements of p^* and r_c.

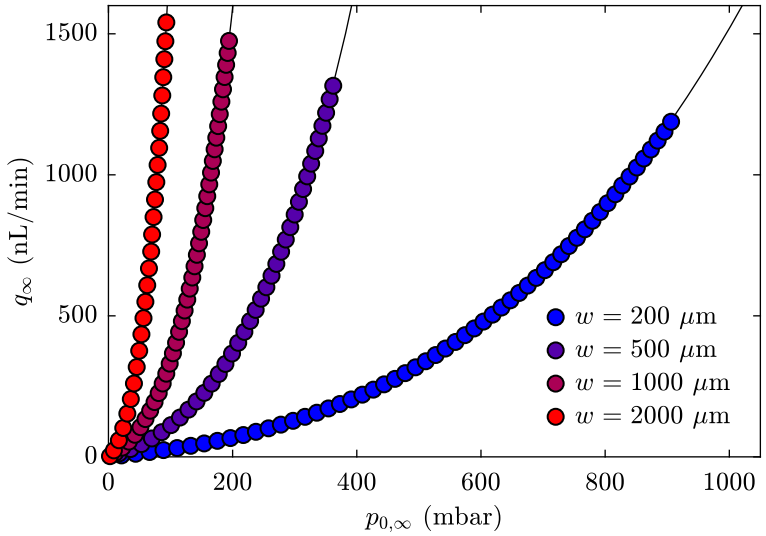

Figure S2. Raw q_∞-*vs.*-$p_{0,\infty}$ data for channels of different widths. The solid lines are fits according to Eq. S1 (*cf.* Eq. 5 in the main text), p^* and r_c being the fitting parameters.

S.IV. SCALING LAWS FOR τ_t AT HIGH AND LOW $P_{0,\infty}$

The relation describing the experimentally measured, transient relaxation time, τ_t, is given by Eq. 8 of the main Letter: $\tau_t = \tau_c/(\lambda_s \Pi^2)$, where λ_s depends on the variables $\Pi, \mathcal{R}, \mathcal{T}$. We also recall that $\Pi = (1+P_{0,\infty})^4 - 1$, and $\mathcal{R}$ and $\mathcal{T}$ are dimensionless parameters describing the resistance and characteristic time scale of peripheral sensors. Furthermore, λ_s is the smallest solution of Eq. 7 from the main Letter, this latter equation determining all the allowed values of λ, and recalled here:

$$\frac{1}{\mathcal{R}\tilde{X_0}^{3/8}}\left(\mathcal{T}\sqrt{\lambda}\Pi - \frac{1}{\sqrt{\lambda}\Pi}\right) = \frac{\mathcal{C}_{-\frac{1}{5}}\left(\frac{8\sqrt{\lambda}}{5}\tilde{X_0}^{5/8}\right)}{\mathcal{C}_{\frac{4}{5}}\left(\frac{8\sqrt{\lambda}}{5}\tilde{X_0}^{5/8}\right)} \ . \tag{S2}$$

We furthermore have $\tilde{X_0} = 1+\Pi$ and $\mathcal{C}_\nu(x) = \mathrm{Y}_{\frac{4}{5}}\left(\frac{8\sqrt{\lambda}}{5}\right)\mathrm{J}_\nu(x) - \mathrm{J}_{\frac{4}{5}}\left(\frac{8\sqrt{\lambda}}{5}\right)\mathrm{Y}_\nu(x)$. This equation is solved numerically in the general case, as exemplified in Fig. S3 for two different values of Π and the noted values of $\mathcal{R}, \mathcal{T}$.

To the best of our knowledge there is no general analytical solution for λ; however, asymptotic scaling laws can be determined in the limits of small and large Π.

Small-Π regime: First, we assume an asymptotic power-law solution, $\lambda_s \approx \beta^2\Pi^\gamma$, when Π goes to zero, with β and γ assumed to be independent of Π. Here we demonstrate the physical intuition described in the main Letter that suggests $\gamma = -2$ and thus a time scale independent of the pressure; we also provide an implicit relation for the constant prefactor β.

For $\Pi \ll 1$, we have $\tilde{X_0} \approx 1$; inserting the power-law ansatz, furthermore, the left-hand side of Eq. S2 can be approximated as:

$$\frac{1}{\mathcal{R}\tilde{X_0}^{3/8}}\left(\mathcal{T}\sqrt{\lambda}\Pi - \frac{1}{\sqrt{\lambda}\Pi}\right) \approx \frac{1}{\mathcal{R}}\left(\mathcal{T}\beta\Pi^{1+\frac{\gamma}{2}} - \frac{1}{\beta\Pi^{1+\frac{\gamma}{2}}}\right). \tag{S3}$$

For the right-hand side of the eigenvalue relation Eq. S2, and as is suggested by the data of Fig. S3(a), we assume that $\lambda_s \to \infty$ when $\Pi \to 0$. Under this hypothesis, we have the argument of the Bessel functions $\sqrt{\lambda}\tilde{X_0}^{5/8} \to \infty$, such that we can use the asymptotic developments of Bessel functions at infinity. Namely, for any complex number z: $\mathrm{J}_\nu(z) \approx \sqrt{\frac{2}{\pi z}}\cos\left(z - \frac{\nu\pi}{2} - \frac{\pi}{4}\right)$ and $\mathrm{Y}_\nu(z) \approx \sqrt{\frac{2}{\pi z}}\sin\left(z - \frac{\nu\pi}{2} - \frac{\pi}{4}\right)$. Using these formulas, the definition of $\mathcal{C}_\nu$, and basic trigonometric sum identities, we obtain:

$$\mathcal{C}_\nu\left(\frac{8\sqrt{\lambda}}{5}\tilde{X_0}^{5/8}\right) \approx \frac{5}{4\pi\sqrt{\lambda}}\tilde{X_0}^{-5/16}\sin\left(\frac{8}{5}\sqrt{\lambda}\left(1-\tilde{X_0}^{5/8}\right) + \frac{5\nu-4}{10}\pi\right) \ .$$

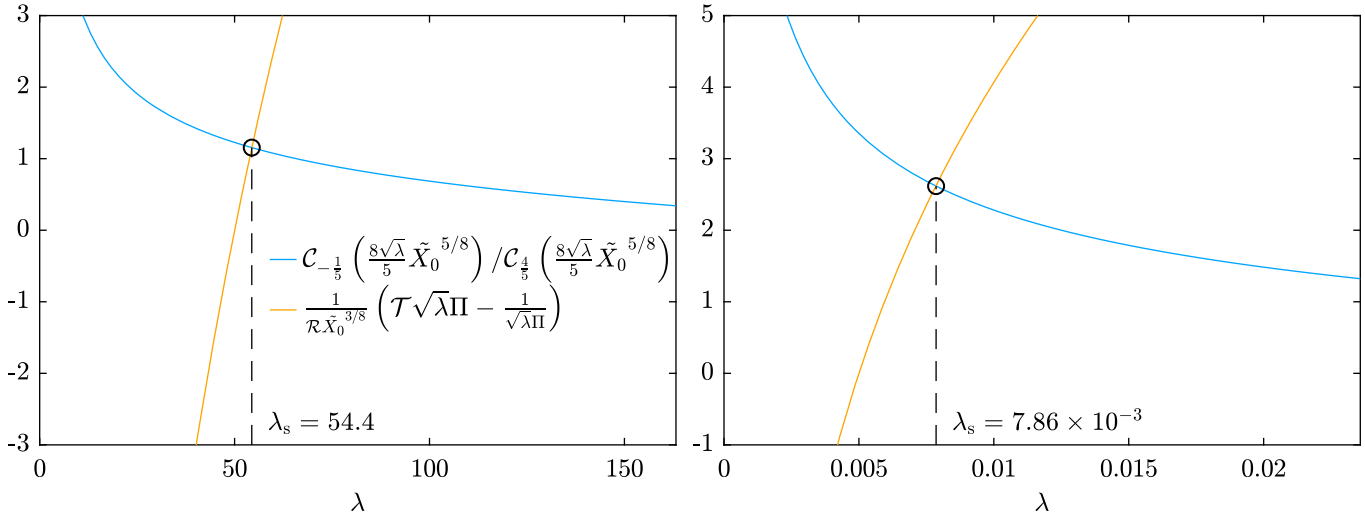

Figure S3. Numerical resolution of Eq. 7 of the main Letter, with **(a)** {Π,$\mathcal{T}$,$\mathcal{R}$}={0.1,2,0.1} and **(b)** {Π,$\mathcal{T}$,$\mathcal{R}$}={10,2,0.1}

Thus we have:

$$\frac{\mathcal{C}_{-\frac{1}{5}}\left(\frac{8\sqrt{\lambda}}{5}\tilde{X_0}^{5/8}\right)}{\mathcal{C}_{\frac{4}{5}}\left(\frac{8\sqrt{\lambda}}{5}\tilde{X_0}^{5/8}\right)} \approx \frac{\sin\left(\frac{8}{5}\sqrt{\lambda}\left(1-\tilde{X_0}^{5/8}\right)-\frac{\pi}{2}\right)}{\sin\left(\frac{8}{5}\sqrt{\lambda}\left(1-\tilde{X_0}^{5/8}\right)\right)} \approx -\mathrm{cotan}\left(\frac{8}{5}\sqrt{\lambda}\left(1-\tilde{X_0}^{5/8}\right)\right). \tag{S4}$$

Developing the argument inside the cotan function, we have $\frac{8}{5}\sqrt{\lambda}\left(1-\tilde{X_0}^{5/8}\right) \approx -\beta\Pi^{1+\frac{\gamma}{2}}$, and finally combining Eq. S2, S3 and S4 we obtain:

$$\frac{1}{\mathcal{R}}\left(\mathcal{T}\beta\Pi^{1+\frac{\gamma}{2}} - \frac{1}{\beta\Pi^{1+\frac{\gamma}{2}}}\right) \approx \mathrm{cotan}\left(\beta\Pi^{1+\frac{\gamma}{2}}\right). \tag{S5}$$

To satisfy the hypothesis that β is independent of Π, it must be that $\gamma = -2$, verifying the assumption that $\lambda_\mathrm{s} \to \infty$ when $\Pi \to 0$. Then assuming equality of the limits of the two sides of Eq. S2, we obtain the following equation on β.

$$\mathcal{T}\beta^2 - \mathcal{R}\beta\mathrm{cotan}(\beta) - 1 = 0. \tag{S6}$$

This equation always has a positive solution for $\beta \in [0, \pi]$, provided $\mathcal{R} > 0$. Thus the scaling hypothesis is valid, and we have $\tau_\mathrm{t} = \tau_\mathrm{c}/\beta^2$.

Large-Π regime: We now turn our attention to the large-Π case. Again we assume a power law behavior of the form $\lambda_\mathrm{s} \approx \beta^2\Pi^\gamma$ when Π goes to infinity. Due to the vanishing resistance of the channel on large deformation, it is expected that $\tau_\mathrm{t} \sim \frac{1}{\lambda_\mathrm{s}\Pi^2} \to 0$ at large Π; therefore, we assume that $\gamma > -2$. In this case $\sqrt{\lambda}\Pi \to \infty$, and we have:

$$\frac{1}{\mathcal{R}\tilde{X_0}^{3/8}}\left(\mathcal{T}\sqrt{\lambda}\Pi - \frac{1}{\sqrt{\lambda}\Pi}\right) \approx \frac{\mathcal{T}}{\mathcal{R}}\beta\Pi^{\frac{1}{8}(4\gamma+5)}. \tag{S7}$$

Substituting the power-law behavior for λ_s in the right-hand-side of Eq. S2, we obtain:

$$\frac{\mathcal{C}_{-\frac{1}{5}}\left(\frac{8\sqrt{\lambda}}{5}\tilde{X_0}^{5/8}\right)}{\mathcal{C}_{\frac{4}{5}}\left(\frac{8\sqrt{\lambda}}{5}\tilde{X_0}^{5/8}\right)} \approx \frac{\mathcal{C}_{-\frac{1}{5}}\left(\frac{8}{5}\beta\Pi^{\frac{1}{8}(4\gamma+5)}\right)}{\mathcal{C}_{\frac{4}{5}}\left(\frac{8}{5}\beta\Pi^{\frac{1}{8}(4\gamma+5)}\right))}. \tag{S8}$$

Then, combining Eqs. S2, S7 and S8, we have:

$$\frac{\mathcal{T}}{\mathcal{R}}\beta\Pi^{\frac{1}{8}(4\gamma+5)} \approx \frac{\mathcal{C}_{-\frac{1}{5}}\left(\frac{8}{5}\beta\Pi^{\frac{1}{8}(4\gamma+5)}\right)}{\mathcal{C}_{\frac{4}{5}}\left(\frac{8}{5}\beta\Pi^{\frac{1}{8}(4\gamma+5)}\right)}. \tag{S9}$$

As in the small-Π case, Eq. S9 suggests that $\gamma = -5/4 > -2$ (the latter inequality as initially assumed) is a solution for the power-law ansatz; it thus remains to verify the independence of β from Π.

Choosing the value of γ thus suggested, we have $\frac{8\sqrt{\lambda}}{5}\tilde{X_0}^{5/8} \to \frac{8\beta}{5}$ in the large pressure limit. Furthermore, as also suggested by the data in Fig. S3, we use developments of the Bessel functions as λ goes to zero for large Π. Therefore,

$$\mathrm{J}_{\frac{4}{5}}\left(\frac{8\sqrt{\lambda}}{5}\right) \approx \frac{1}{\Gamma(9/5)}\left(\frac{4\sqrt{\lambda}}{5}\right)^{4/5} \quad , \quad \mathrm{Y}_{\frac{4}{5}}\left(\frac{8\sqrt{\lambda}}{5}\right) \approx -\frac{\Gamma(4/5)}{\pi}\left(\frac{5}{4\sqrt{\lambda}}\right)^{4/5} ,$$

and we have

$$\mathcal{C}_{-\frac{1}{5}}\left(\frac{8\sqrt{\lambda}}{5}\tilde{X_0}^{5/8}\right) \approx -\frac{\Gamma(4/5)}{\pi}\left(\frac{5}{4\sqrt{\lambda}}\right)^{4/5}\mathrm{J}_{-\frac{1}{5}}\left(\frac{8\beta}{5}\right) \quad , \quad \mathcal{C}_{\frac{4}{5}}\left(\frac{8\sqrt{\lambda}}{5}\tilde{X_0}^{5/8}\right) \approx -\frac{\Gamma(4/5)}{\pi}\left(\frac{5}{4\sqrt{\lambda}}\right)^{4/5}\mathrm{J}_{\frac{4}{5}}\left(\frac{8\beta}{5}\right) ,$$

such that we finally have:

$$\frac{\mathcal{C}_{-\frac{1}{5}}\left(\frac{8\sqrt{\lambda}}{5}\tilde{X_0}^{5/8}\right)}{\mathcal{C}_{\frac{4}{5}}\left(\frac{8\sqrt{\lambda}}{5}\tilde{X_0}^{5/8}\right)} \approx \frac{\mathrm{J}_{-\frac{1}{5}}\left(\frac{8\beta}{5}\right)}{\mathrm{J}_{\frac{4}{5}}\left(\frac{8\beta}{5}\right)}. \tag{S10}$$

With $\gamma = -5/4$ as suggested by Eq. S9, combining Eqs. S2, S7, and S10 and using the uniqueness of the limit, we obtain the following condition on β in the large-pressure limit:

$$\frac{\mathcal{T}}{\mathcal{R}}\beta = \frac{\mathrm{J}_{-\frac{1}{5}}\left(\frac{8\beta}{5}\right)}{\mathrm{J}_{\frac{4}{5}}\left(\frac{8\beta}{5}\right)} \,. \tag{S11}$$

A simple analysis of the function $z \to \mathrm{J}_{-1/5}(z)/\mathrm{J}_{4/5}(z)$ shows that Eq. S11 always has a real solution, which validates the hypothesis on the scaling. We finally have $\tau_\mathrm{t} = \tau_\mathrm{c}\Pi^{-3/4}/\beta^2 = \tau_\mathrm{c}/(\beta^2 P_{0,\infty}^3)$ for large pressures, as suggested in the manuscript.

S.V. FLOW SENSOR CALIBRATION

In Fig. S4 is shown the steady-state response of the flow sensor, *i.e.* q_∞ as a function of $p_{\mathrm{in},\infty}$, as taken from the plateau values of the data in Fig. S1(a). The data is well described by a straight line of slope 2.40 nL/ min /mbar, which corresponds to a hydraulic resistance of 2.50 ± 0.01 kPa nL^{-1}. This value is consistent with the resistance of a capillary of internal diameter 25 µm and length 2.4 cm, used with a fluid of viscosity 1.0 mPa s. The linearity of the data also indicates the negligible compliance of the flow sensor in the accessible range of pressures.

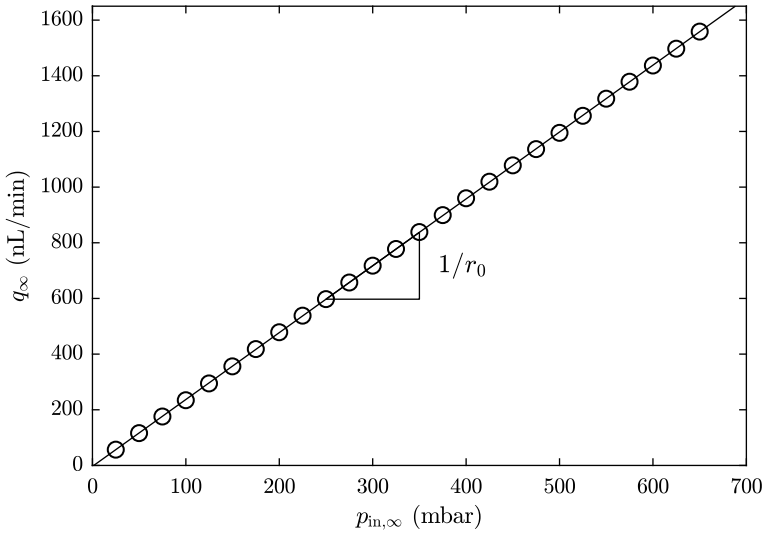

Figure S4. Flow sensor calibration: q_∞ as a function of $p_{\mathrm{in},\infty}$ for the case of a pressure controller and flow sensor only. The solid black line is a linear regression of the data, the slope of which provides a measurment of r_0.

* joshua.mcgraw@cnrs.fr